University of South Carolina

Scholar Commons

7-30-2018

Nickel Exposure Reduces Enterobactin Production in *Escherichia coli*

Clorissa L. Washington-Hughes
University of South Carolina - Columbia

Geoffrey T. Ford
University of South Carolina - Columbia

Alsten D. Jones
University of South Carolina - Columbia

Kimberly McRae
University of South Carolina - Columbia

Franklin Wayne Outten
University of South Carolina - Columbia, outtenf@mailbox.sc.edu

Follow this and additional works at: https://scholarcommons.sc.edu/chem_facpub

Part of the Biochemistry, Biophysics, and Structural Biology Commons, and the Chemistry Commons

Publication Info
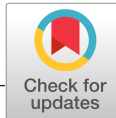
WILEY MicrobiologyOpen

Nickel exposure reduces enterobactin production in *Escherichia coli*

Clorissa L. Washington – Hughes | Geoffrey T. Ford | Alsten D. Jones | Kimberly McRae | F. Wayne Outten [ID]

Department of Chemistry and Biochemistry, University of South Carolina, Columbia, South Carolina

Correspondence
F. Wayne Outten, Department of Chemistry and Biochemistry, University of South Carolina, Columbia, SC.
Email: outtenf@mailbox.sc.edu

Abstract

Escherichia coli is a well-studied bacterium that can be found in many niches, such as industrial wastewater, where the concentration of nickel can rise to low-millimolar levels. Recent studies show that nickel exposure can repress pyochelin or induce pyoverdine siderophore production in *Pseudomonas aueroginosa*. Understanding the molecular cross-talk between siderophore production, metal homeostasis, and metal toxicity in microorganisms is critical for designing bioremediation strategies for metal-contaminated sites. Here, we show that high-nickel exposure prolongs lag phase duration as a result of low-intracellular iron levels in *E. coli*. Although *E. coli* cells respond to low-intracellular iron during nickel stress by maintaining high expression of iron uptake systems such as *fepA*, the demand for iron is not met due to a lack of siderophores in the extracellular medium during nickel stress. Taken together, these results indicate that nickel inhibits iron accumulation in *E. coli* by reducing the presence of enterobactin in the extracellular medium.

KEYWORDS

enterobactin, *Escherichia coli*, iron, nickel, siderophore

1 | INTRODUCTION

Siderophores are small molecules with high affinity for ferric iron and are produced by bacteria under iron-limiting conditions (Matthew, Jenul, Carlier, & Eberl, 2016; Neilands, 1995). Siderophores are exported from the cell into the extracellular environment to bind and transport ferric iron (Fe^{3+}) back into the cell. Siderophores have also been shown to promote intracellular iron accumulation in *Pseudomonas aeruginosa* (Braud, Geoffroy, Hoegy, Mislin, Schalk, 2010), alter metal toxicity in uropathogenic bacteria (Chaturvedi, Hung, Crowley, Stapleton, & Henderson, 2012), protect against oxidative stress (Adler et al., 2014), and detoxify metal-contaminated soils (Nair, 2007).

Enterobactin is the predominant siderophore secreted by *E. coli* under iron-limiting conditions. Niches where those conditions exist include soil (Solomon, Yaron, & Matthews, 2002), plants (Itoh et al., 1998), and mammalian intestinal systems or pathogenesis sites (Van Elsas, Semenov, Costa, & Trevors, 2011). In *E. coli*, enterobactin is synthesized by the concerted action of the gene products encoded by the *entCEBA* operon (Crosa & Walsh, 2002; Ma & Payne, 2012; Walsh, Liu, Rusnak, & Sakaitani, 1990). It is then exported from the cytoplasm by the inner membrane transporter protein EntS (Bleuel et al., 2005; Furrer, Sanders, Hook-Barnard, & McIntosh, 2002; Miethke & Marahiel, 2007). Extracellular ferric iron binds to apo-enterobactin forming Fe^{3+}–enterobactin. Fe^{3+}–enterobactin is preferentially imported back into the cell by binding to the outer membrane transporter protein FepA, then to FepB in the periplasm, and through the FepCDG transporter in the inner membrane (Braun, 1995; Larsen, Foster-Hartnett, McIntosh, & Postle, 1997). Enterobactin is the

cyclized form of three N-(2, 3-dihydroxybenzoyl)-L-serine mono-meric units (Ehmann, Shaw-Reid, Losey, & Walsh, 2000; Gehring, Bradley, & Walsh, 1997; Gehring, Mori, & Walsh, 1998; Shaw-Reid et al., 1999). The backbone of intracellular Fe^{3+}–enterobactin must be hydrolyzed by the esterase Fes and the iron reduced by YqjH (NfeF), releasing ferrous iron from the tightly chelated ferric complex (Brickman & McIntosh, 1992; Bryce & Brot, 1972; Greenwood & Luke, 1978; Langman, Young, Frost, Rosenberg, & Gibson, 1972; Miethke, Hou, & Marahiel, 2011). The cleavage of intracellular enterobactin (cyclo-tris(2,3-dihydroxy-N-benzoylseryl) by Fes results in the production of four linear hydrolysis products including: the non-hydrolytically cleaved trimer (N, N', N''-tris(2,3-dihydroxybenzoyl)-O-(a-aminoacrylyl)-O-seryl serine), the hydrolytically cleaved trimer (N, N', N'''-tris(2,3-dihydroxybenzoyl)-O-seryl-O-seryl serine), a linear dimer (N, N'-bis(2,3-dihydroxybenzoyl)-O-(a-aminoacrylyl)-O-seryl serine), and a linear monomer (2,3-dihydroxy-N-benzoylserine) (Lin, Fischbach, Liu, & Walsh, 2005; Brickman & McIntosh, 1992; O'Brien & Gibson, 1970).

Siderophores like enterobactin have been shown to impact homeostasis of other essential or toxic metals. For example, enterobactin can facilitate the reduction in Cu^{2+} to Cu^{1+} and increase copper cytotoxicity in uropathogenic _E. coli_ (Chaturvedi et al., 2012). Siderophores have been shown to protect against metal toxicity perhaps by chelating other metals (Chen, Jurkewitch, Bar-Ness, & Hadar, 1994; Koh et al., 2015). The presence of the _Pseudomonas aeruginosa_ siderophores pyochelin (PCH) and pyoverdine (PVD) have been shown to decrease intracellular nickel accumulation (Braud, Hannauer, Mislin, & Schalk, 2009; Braud, Hoegy, Jezequel, Lebeau, & Schalk, 2009; Braud et al., 2010). In addition, media supplementation with PCH and PVD reduced nickel toxicity in iron-limited and iron-supplemented media (Braud et al., 2010). However, exposure to other toxic metals can also alter siderophore expression. Siderophore production is repressed by excess molybdenum in _Azobacter vinelandii_ (Duhme, Hider, Naldrett, & Pau, 1998) but aluminum increases hydroxamate siderophore production in _Bacillus megaterium_ (Hu & Boyer, 1996). Copper and nickel can increase siderophore production in the presence of iron levels that are not limiting for growth in _Pseudomonas aeruginosa_ (Braud et al., 2010; Visca et al., 1992). In _P. aeruginosa_, nickel has been shown to repress PCH synthesis (Visca et al., 1992) but induce PVD synthesis (Braud, Hannauer, Mislin, & Schalk, 2009) under iron-limited conditions. Therefore, understanding the molecular cross-talk between siderophore production, metal homeostasis, and metal toxicity in microorganisms is critical for designing bioremediation strategies for metal-contaminated sites (Dixit et al., 2015). For example, Actinobacteria can be used to detoxify metal-contaminated sites and break-down complex organic matter (Albarracín, Amoroso, & Abate, 2005; Alvarez et al., 2017; Kieser, Bibb, Buttner, Chater, & Hopwood, 2000; Polti, Amoroso, & Abate, 2011; Polti, Aparicio, Benimeli, & Amoroso, 2014; Polti, Atjian, Amoroso, & Abate, 2011; Polti, García, Amoroso, & Abate, 2009). Its robust metabolic profile and the emergence of new actinobacteria species (Kaewkla & Franco, 2013) has made this class of organism a prime system for

understanding the molecular details of siderophore production (Wang, Qiu, Tan, & Cao, 2014).

Recently, nickel has been shown to lower intracellular iron concentrations possibly by transcriptional repression of iron acquisition genes in _E. coli_ (Gault, Effantin, & Rodrigue, 2016). Furthermore, strains lacking the stress-responsive iron cofactor biogenesis system Suf are more sensitive to nickel stress than wild-type _E. coli_ (Wang, Wu, & Outten, 2011). Our goal in this work is to test if nickel stress alters siderophore production under iron-limiting conditions in _E. coli_.

2 | EXPERIMENTAL PROCEDURES

2.1 | Bacterial strains and culture conditions

Strains used in this study are derivatives of the parent wild-type strain _E. coli_ MG1655. An individual colony was transferred from fresh Lennox broth (LB) agar plates into a 4 ml volume of LB and grown for 4-5 hr at 37°C with shaking at 200 rpm. Cells from this culture were pelleted and washed twice in sterile 1X M9 minimal media salts; then the $OD_{600\,nm}$ was normalized to 1.0. Normalized cells were diluted 1:200 into M9 glucose minimal media containing 1X M9 minimal salts (BD Difco), 0.2% (w/v) glucose (Acros Organics), 0.2% (w/v) magnesium chloride, 0.1 mM calcium sulfate, and 0.5 g/ml Thiamine HCl (Sigma-Aldrich). Prepared M9 media typically contained ~300 nM iron and ~70 nM nickel as measured by ICP-MS. Cultures were incubated overnight for 18-20 hr, at 37°C and 200 rpm, then washed and pelleted twice in sterile 1X M9 salts as described above. The resulting cell suspensions were normalized to an OD_{600} of 2.0 and diluted 1:50 into M9 gluconate minimal media with 0.2% (w/v) potassium gluconate (Alfa Aesar) to give an initial OD_{600} of 0.04. Nickel chloride (Sigma-Aldrich) was added to describe final concentrations in the M9 gluconate minimal media, from 0 μM up to 50 μM.

Cell growth was monitored as optical density at 600 nm (OD_{600}) and plotted versus time (in hours). Lag phase duration was determined using the online fitting program, DMFit (www.ifr.ac.uk/safety/DMfit), applying the no-asymptote fitted model and parameters (Baranyi & Roberts, 1994). Stationary phase OD_{600} measurements were omitted for best fit of the model. Doubling time of the cells during the exponential phase of growth, where the steepest linear fit line could be applied, was determined using the Online Doubling Calculator (http://www.doubling-time.com/compute.php) (Roth, 2006).

2.2 | Inductively – coupled Plasma Mass Spectrometry (ICP-MS)

Preparatory cell growth in LB and glucose minimal media was conducted as described above. Cell cultures were then grown in 2 L M9 gluconate minimal media with or without 50 μM nickel chloride in a 4 L culture flask at 37°C and 200 rpm. A total of 150 ml samples were centrifuged at 3,000g for 20 min and then pelleted three times

at 16,000g with intermediate washing in 1 ml sterile, ice-cold wash solution consisting of 50 mM EDTA tetrasodium salt, 100 mM oxalic acid, 100 mM NaCl, and 10 mM KCl, to remove any cell surface-associated metal ions. Washed cell pellets were resuspended in a 1 ml volume of ice-cold, sterile 1X M9 salts. A small portion of each sample was then diluted 40-fold to record the final OD_{600}. Cell resuspensions were transferred to an acid-washed, Perfluoroalkoxy (PFA) microcentrifuge tube (Savillex Corporation) and centrifuged at 16,000g. After centrifugation, the supernatant was discarded and the cell pellets were frozen in liquid nitrogen. Cell pellets were stored at −80°C until ready for digestion and ICP-MS analysis.

Samples for ICP-MS were thawed for 15 min on ice followed by drying at 80°C for 30 min. A 400 μL volume of trace-metal grade HNO_3 (distilled on site at the Center for Elemental Mass Spectrometry (CEMS), University of South Carolina) was added to each sample tube and digested at 80°C for 4 hr. After digestion, each sample tube was centrifuged for 1 min at 16,000g and the supernatant was diluted 1:20 into MQ H_2O, giving a final acid matrix of 3.5%. Blanks consisting of 3.5% trace-metal grade HNO_3 only in MQ H_2O (18MΩ) were made and prepared in the same manner as the cell samples. Standard element solutions (Inorganic Ventures) were also prepared in the same final acid matrix of 3.5% to establish a limit of detection and a calibration curve for determining the concentrations of each metal analyzed. The isotopes of biologically relevant transition metals with masses of ^{56}Fe, ^{58}Ni, ^{64}Zn, ^{55}Mn, and ^{63}Cu were selected for analysis based on natural abundances. Samples were analyzed under medium resolution to resolve polyatomic interferences (e.g. $^{40}Ar^{16}O$ for ^{56}Fe) on a Thermo Element 2 High Resolution ICP-MS instrument operated by CEMS at the University of South Carolina. A cyclonic spray chamber (Elemental Scientific) was used for delivery of sample into the instrument.

2.3 | β-Galactosidase assays for promoter-lacZ fusion strains

Wild-type _E. coli_ MG1655 strains containing Φ_fepAp-LacZ_ (PK9849), Φ_iscRp-lacZ_ (PK7571), and Φ_sufAp-lacZ_ (PK7722) were kindly provided by Patricia Kiley (University of Wisconsin – Madison) (Giel, Rodionov, Liu, Blattner, & Kiley, 2006). All cells were initially plated on LB with 30 μg/ml kanamycin overnight at 37°C. One colony was transferred to M9 glucose minimal media for approximately 18 hr at 37°C at 200 rpm. The cell culture was then diluted 1:50 to a final OD_{600} of 0.04 in 100 ml of M9 gluconate minimal media with or without 50 μM $NiCl_2$ and grown for 5 hr at 37°C at 200 rpm. At various time points, cells were collected by centrifugation at 3,000g and resuspended in Z-buffer (0.06 M sodium diphosphate, 0.04 M monosodium phosphate, 0.01 M potassium chloride, 0.001 M magnesium sulfate, and 0.05 M β-mercaptoethanol). β-galactosidase activity was measured after addition of 200 μl of 4 mg/ml ortho-Nitrophenyl-ß-galactoside per ml of cells permeabilized with chloroform and SDS according to published protocols (Miller, 1972). β-galactosidase activity was calculated and reported in

Miller Units; see Equation 1 below where t = time of reaction and υ = volume of cells added in ml. Absorbance at 420 nm, 550 nm, and 600 nm were measured using a Beckman-Coulter DU800 UV-Vis Spectrophotometer. Miller units normalize β-galactosidase activity to total cell number via optical density at 600 nm (OD_{600}) measurement.

$$\text{Miller Unit} = 1000 * [Abs_{420} - (1.75 * Abs_{550})]/[t * \upsilon * Abs_{600} \tag{1}$$

2.4 | Arnow assay for catechol determination

Methods from Arnow and Ma were adapted for the quantitation of catecholate siderophore production (to include any enterobactin breakdown products) by _E. coli_ under nickel stress (Arnow, 1937; Ma & Payne, 2012). Wild-type MG1655 and Δ_fepA_ strains were cultured as described above. Cells were cultured in 0.2% gluconate M9 minimal media with or without 50 μM nickel chloride. Every 2 hr 1 ml was collected from each growth, the OD at 650 nm was measured and recorded, and then each volume was cleared of cells via centrifugation at 16,000g for 1 min. A 500 μl volume of cleared supernatant was transferred to a clean, 4.0 ml polypropylene cuvette. A total of 500 μl 0.5N HCl, 500 μl of a 10% sodium nitrate/10% sodium molybdate mixture (Sigma-Aldrich), and 500 μl 1N NaOH were added to the cuvette. All assay samples were measured against a blank mixture of fresh gluconate M9 minimal media with the above reagents listed for the assay. The absorbance at 515 nm was measured and recorded immediately after mixing. Arnow units were calculated using Equation 2

$$\text{Arnow Unit} = 1000 * [Abs_{515}/Abs_{650}] \tag{2}$$

2.5 | Enterobactin purification and quantitation using FPLC

Escherichia coli MG1655 wild-type and Δ_fepA_ were plated onto LB and incubated overnight at 37°C. A single colony was cultured according as described above. Cultured cells were washed, normalized, and diluted to a final optical density of 0.04 in M9 gluconate minimal media, with or without 50 μM nickel chloride. Cultures were incubated for 2 hr at 37°C at 200 rpm. The cells were centrifuged for 20 min at 4°C and 8,000g. The supernatant was sterile filtered twice using a fresh 0.22 μm filter (Millipore) each time and a total of 1 L spent media was collected. Enterobactin and its hydrolysis products were purified using a modified form of a previously published protocol (O'Brien & Gibson, 1970). Briefly, the sterile, filtered supernatant was loaded onto a DEAE-Sepharose Fast Flow column equilibrated with 10 mM sodium phosphate buffer, pH 7.0. 5 ml fractions were collected by eluting at 4°C using a step gradient of 0.0 M, 0.05 M, 0.15 M, 1.0 M, and 2.0 M ammonium chloride. Enterobactin and its hydrolysis products were identified based on the concentration of ammonium chloride

at which they eluted and further confirmed by ESI-MS (data not shown).

3 | RESULTS

3.1 | Wild-type *E. coli* cells are sensitive to nickel stress during lag phase

Escherichia coli cells have three primary stages of growth: lag phase, exponential phase, and stationary phase (Wade, 1952). Nickel is toxic at low micromolar levels (8 μM) to bacterial cells in exponential phase and nickel was shown to disrupt the zinc-dependent metalloenzyme Class 2 Fructose-bisphosphate aldolase, FbaA (Macomber, Elsey, & Hausinger, 2011). Nickel exposure in exponential phase *E. coli* was also shown to induce DNA relaxation and damage, possibly by inhibiting DNA replication and RecBCD-mediated DNA repair rather than by generating reactive oxygen species (Gault et al., 2016 and Kumar, Mishra, Kaur, & Dutta, 2017). However, Rolfe et al., (2012) have shown that bacterial cells accumulate essential trace metals during *lag phase* in preparation for the transition into exponential phase. Iron uptake genes are upregulated and intracellular iron levels are increased during lag phase. During exponential phase, these genes are downregulated and intracellular iron levels decrease as the iron is progressively divided among daughter cells. To determine the effects of nickel during lag phase of *E. coli*, growth was monitored after exposure of freshly diluted lag phase cells to 0–50 μM nickel chloride (Figure 1a). Lag phase duration (Figure 1b) was quantitated using the Baranyi and Roberts model (Baranyi & Roberts, 1994) while the exponential phase (doubling time) duration (Figure 1c) was quantitated using a formula developed by Roth (2006). Lag phase duration is not significantly affected at the lower nickel toxicity range (below 10 μM). However, as the concentration of nickel increases above 10 μM, lag phase duration also increases. The doubling time does not significantly change when the nickel-treated cells exit lag phase and enter exponential phase. Similarly, the final cell density reached in stationary phase also does not significantly change after nickel exposure in lag phase (Figure 1a).

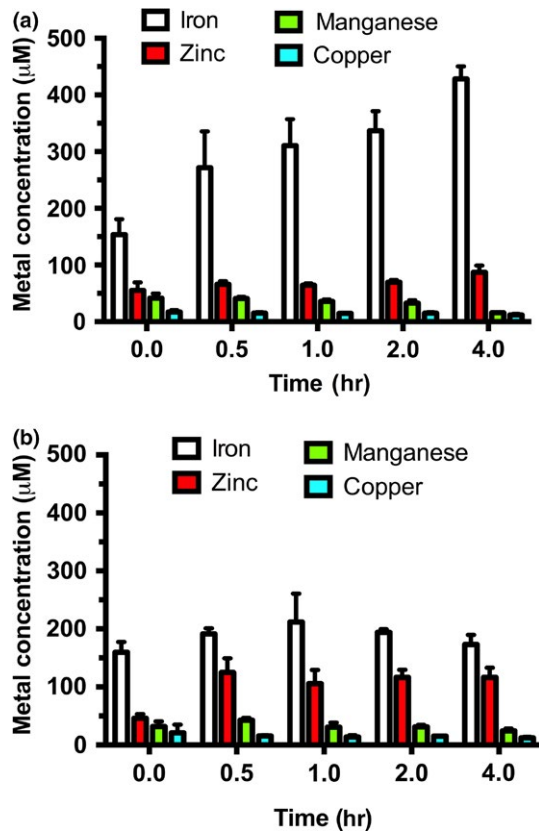### 3.2 | Intracellular iron levels are lower in nickel-treated *E. coli* cells

Soft metals have been shown to disrupt iron metabolism in *E. coli* (Macomber & Imlay, 2009; Ranquet, Ollagnier-de-Choudens, Loiseau, Barras, & Fontecave, 2007; Xu & Imlay, 2012). Recent studies link nickel stress to disruption of iron metabolism in exponential phase, possibly by inducing Fur-dependent repression of iron uptake systems (Gault et al., 2016). To better understand the phenotypic effects of nickel toxicity, intracellular metal concentrations during lag phase nickel stress were measured using inductively coupled plasma mass spectrometry (ICP-MS). Cells that were not exposed to nickel showed an increasing amount of iron over time during lag phase (Figure 2a). In contrast, cells exposed to a toxic level of nickel (50 μM) showed no increase in intracellular iron throughout
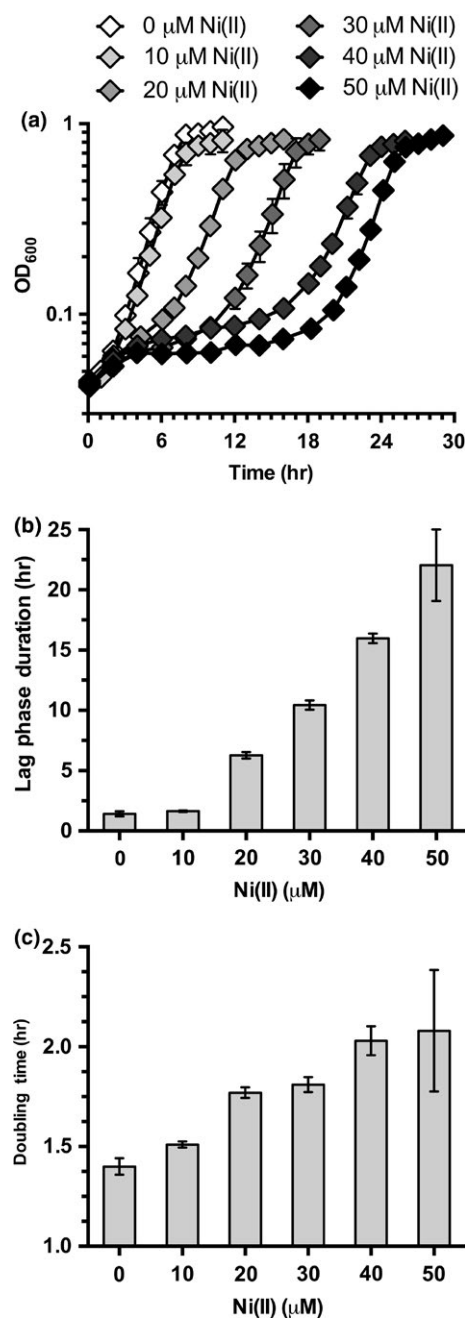
FIGURE 1 Nickel exposure extends lag phase duration. (a) Growth curves of wild type MG1655 *Escherichia coli* cells in M9 gluconate minimal media exposed to 0 μM, 10 μM, 20 μM, 30 μM, 40 μM, or 50 μM nickel chloride. (b) Lag phase duration calculated from the growth curve data shown in (a). (c) Doubling times calculated from the growth curve data shown in (a). All growths were repeated in triplicate (n = 3) and error bars indicate one standard deviation from the mean value

lag phase but did accumulate nickel (Figure 2b and S1). Manganese and copper levels were not significantly affected but zinc levels were elevated in response to nickel. The increased zinc accumulation in response to nickel is consistent with disruption of zinc metalloproteins by nickel as previously reported (Macomber & Hausinger, 2011; Macomber et al., 2011).

FIGURE 2 Intracellular iron levels are decreased upon exposure to nickel during the lag phase. (a) Intracellular metal concentrations were measured in wild type MG1655 *Escherichia coli* cells that were exposed to 0 μM nickel chloride using ICP-MS. (b) Intracellular metal concentrations were measured in wild type MG1655 *E. coli* cells that was exposed to 50 μM nickel chloride using ICP-MS. All measurements were repeated in triplicate (*n* = 3) and error bars indicate one standard deviation from the mean value

3.3 | High nickel exposure triggers an 'iron starvation' response in lag phase *E. coli* cells

To determine the effects of nickel exposure on intracellular iron homeostasis, expression of genes involved in iron homeostasis were monitored using a series of promoter-*lacZ* fusion constructs in vivo. Iron uptake (*fepA*) and iron-sulfur (Fe-S) cluster biogenesis (*iscR*, *sufA*) genes are upregulated during lag phase and their expression progressively declines over time in exponential phase (Rolfe et al., 2012). The ferric uptake regulator, Fur, regulates iron homeostasis by repressing the transcription of iron uptake genes under iron replete conditions (Escolar, Perez-Martin, & de Lorenzo, 1998; Hunt, Pettis, & McIntosh, 1994). However, when cellular demand for iron is high, Fur repression of genes like *fepA* and *sufA* that are involved in adaptation to iron starvation is reversed leading to their induction. Under normal growth conditions (in the absence of nickel), we observed that *fepA* and *sufA* gene expression levels gradually decreased over time throughout lag phase (Figure 3a,b). In contrast, nickel exposure (50 μM) results in a consistently high level of *fepA* and *sufA* expression throughout lag phase when compared to cells
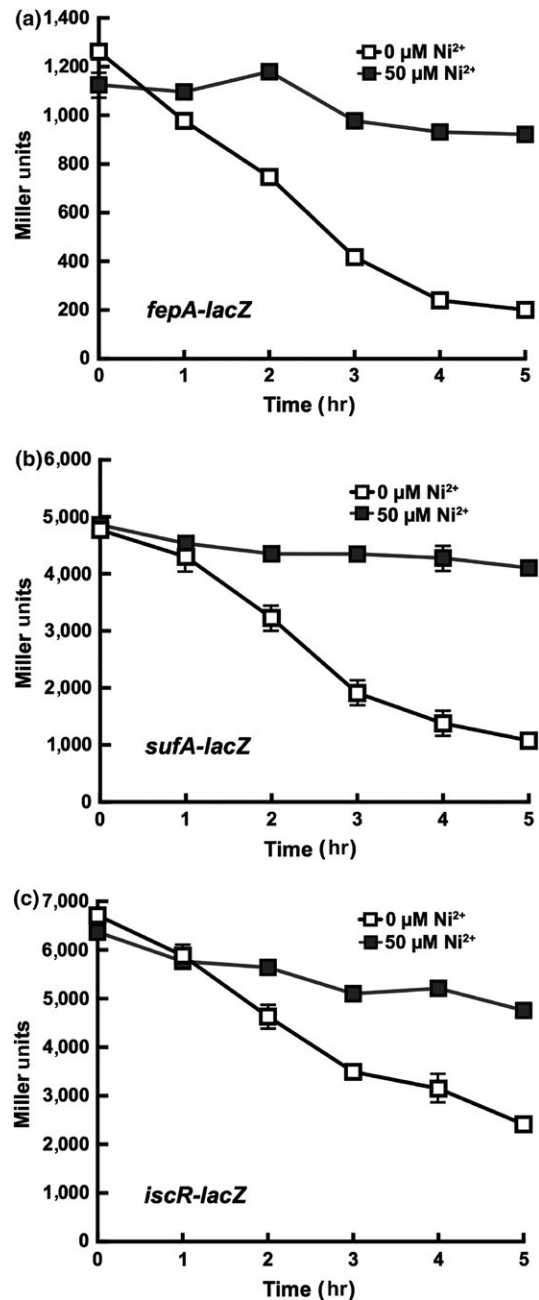
FIGURE 3 Nickel induces the Fur and IscR regulons. Relative gene expression levels are shown in Miller Units which accounts for any observed differences in bacterial cell growth or optical density at 600 nm. (a) *fepA-lacZ* gene expression levels. (b) *sufA-lacZ* gene expression levels. (c) *iscR-lacZ* gene expression levels. All measurements were repeated in triplicate (*n* = 3) and error bars indicate one standard deviation from the mean value

that were not exposed to nickel (Figure 3a,b). The nickel-dependent upregulation of *fepA* in lag phase was also independently confirmed by RT–qPCR (Figure S2). The expression of *iscR* is auto-regulated in response to demand for Fe-S cluster biogenesis and is influenced indirectly by intracellular iron availability. Therefore, *iscR* expression can also be used as an indicator of intracellular iron status. Similar to that observed for *fepA* and *sufA*, *iscR* expression gradually decreased
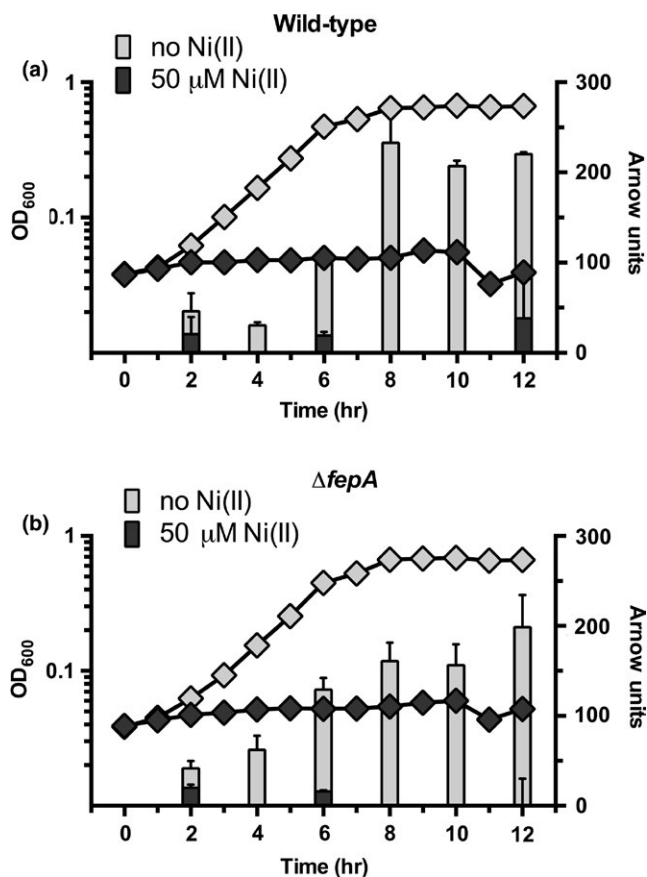
FIGURE 4 Nickel decreases levels of extracellular catecholate siderophores during lag phase. Total catecholate production is expressed in Arnow units (right axis, bars). Relative growth is expressed by optical density at 600 nm (left axis, diamonds). (a) Wild-type and (b) Δ*fepA* MG1655 *E. coli* cells measurements are overlaid with growth data from the same cultures (left axis, diamonds). All growths were repeated in triplicate (*n* = 3) and error bars indicate one standard deviation from the mean value

throughout lag phase in control cells but remained high throughout lag phase in nickel-treated cells (Figure 3c). These results are consistent with other studies and clearly support the hypothesis that nickel disrupts iron metabolism in multiple growth phases in *E. coli* (Gault et al., 2016).

3.4 | The presence of siderophores decreases in nickel-treated *E. coli* cells

When iron is limiting, cells export siderophores into the extracellular environment to chelate ferric iron for transport into the cell. The primary siderophore in the strain of *E. coli* used for these studies is the catechol enterobactin. To assess the effects of nickel on siderophore production, catechol levels were monitored in the culture medium using the Arnow assay (Arnow, 1937; Ma & Payne, 2012). Siderophore production is reported in Arnow units, which are normalized for bacterial cell density. Since they are all catechols, this assay should detect enterobactin and its hydrolysis products if they are present in the extracellular medium. The presence

of catechols in the culture medium gradually increases over time throughout lag and exponential phase in control cells not exposed to nickel (Figure 4a). In contrast, high-nickel stress reduces the catechol accumulation in the culture medium (Figure 4a). The decrease in extracellular siderophore levels was proportional to increasing media nickel concentrations (Figure S3). The siderophore enterobactin is imported by FepA after it chelates extracellular ferric iron. To test if the decrease in extracellular siderophore levels during nickel stress was due to an increased rate of clearance of enterobactin by active import via FepA, catechol production also was measured in a *fepA* deletion mutant strain (Δ*fepA*). Siderophore levels were also lower in Δ*fepA* cells exposed to nickel in comparison to untreated cells (Figure 4b). The Arnow assay cannot differentiate enterobactin from its four hydrolysis products, which can also be secreted into the media as low-affinity iron chelators (Hantke, 1990). To assess the effects of nickel exposure on extracellular enterobactin and its hydrolysis products, fast protein liquid chromatography (FPLC) was used to separate and quantitate enterobactin products from the extracellular medium. In both wild-type and Δ*fepA* strains the presence of enterobactin and all of its hydrolysis products are lower during nickel exposure (Figure 5a,b). A complementary extraction and analysis protocol using ethyl acetate showed a similar trend in nickel-dependent reduction in enterobactin and its hydrolysis products during lag phase (Figure S4).

4 | DISCUSSION

The amount of nickel exposure can proportionally affect the relative growth of *E. coli* cells over time in iron-limited media. The first stage of growth known as lag phase shows a significant impact from nickel exposure (Figure 1a). The lag phase duration of cells exposed to 50 μM nickel chloride is approximately 10-fold longer than cells that were not exposed to nickel stress (Figure 1b). According to Rolfe et al., (2012), lag phase is the stage of growth where bacterial cells accumulate iron. Nickel exposure in lag phase results in lower iron accumulation (Figure 2a) and a cellular iron starvation response where genes required for adaptation to iron starvation are constitutively expressed at high levels during lag phase nickel exposure (Figure 2b). Therefore, the disruption of iron homeostasis by lag phase nickel exposure is in good agreement with other recent studies on iron homeostasis and nickel toxicity (Gault et al., 2016; Rolfe et al., 2012). Interestingly, once nickel-exposed cells exit lag phase, the exponential phase duration (doubling time) shows a much milder twofold increase even at the highest nickel concentration tested. Furthermore, the final cell density reached in stationary phase does not seem to be significantly altered by lag phase nickel exposure (Figure 1a). This result may be partially explained by the selection for a nickel-resistant mutant population during lag phase, which then grows nearly at wild-type rates once they accumulate or exit lag phase. In fact, preliminary studies in our laboratory indicate that a nickel-resistant population is selected for after high-nickel
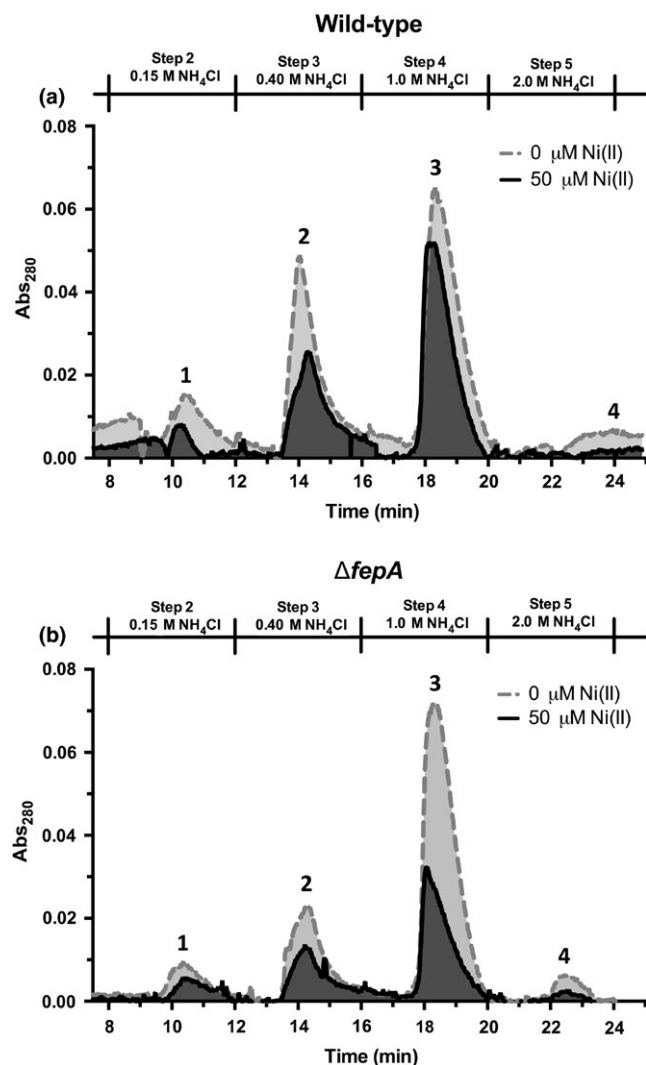
FIGURE 5 Nickel decreases levels of extracellular enterobactin and its hydrolysis products during lag phase (a) Spent media from Wild-type MG1655 culture with 0 μM nickel or 50 μM NiCl$_2$ was filtered and enterobactin-related metabolites were separated by FPLC (b) Spent media from Δ*fepA* cultures with no added nickel or 50 μM NiCl$_2$ was filtered and enterobactin-related metabolites were separated by FPLC. Elution times are shown across the bottom axis. The elution peak annotated '1' refers to the linear dimer, '2' refers to the hydrolytically cleaved linear trimer, '3' refers to the nonhydrolytically cleaved linear trimer, and '4' refers to cyclized enterobactin

exposure in lag phase (at concentrations above 30 μM NiCl$_2$, data not shown).

Despite the demand for iron and the transcriptional upregulation of iron uptake genes, the level of the siderophore enterobactin and all its hydrolysis products are lower in nickel-treated cells as compared to untreated control cells. Previously, it was shown that nickel exposure in exponential phase of growth causes repression of iron uptake pathways, including *fepA* and the *entCEBA* operon used for enterobactin synthesis (Gault et al., 2016). The exact mechanism for this inappropriate repression is not clear but may involve a nickel-dependent increase in intracellular labile iron, perhaps

from damaged or mis-metallated iron proteins, which then triggers inappropriate Fur-dependent repression of target genes. Using the *lacZ* promoter fusion construct for *fepA*, we also observed similar reduced expression during *exponential* phase nickel exposure (data not shown). However, expression of both *fepA* and *entC* is constitutively high during *lag* phase nickel exposure, as measured by *lacZ* promoter fusions and RT-qPCR (Figure 3 and S2). Therefore, transcriptional repression of the *entCEBA* system does not explain the observed reduction in enterobactin in the media during lag phase nickel exposure.

Taken together, these findings support the notion that high nickel exposure can disrupt siderophore production in *E. coli* as was previously reported in *Pseudomonas aeruginosa* under iron-limiting conditions (Visca et al., 1992). These results may provide an additional mechanism to help explain the observed drop in iron accumulation under nickel stress seen in *E. coli* grown under aerobic conditions in minimal media (Gault et al., 2016). Under those growth conditions where ferric iron predominates, the enterobactin uptake pathway would be the main route for iron entry into the cell. However, the results we obtained in lag phase also point to some distinct differences in nickel-mediated disruption of iron homeostasis between lag and exponential growth phases. In lag phase, the reduction in iron accumulation is much more severe and the Fur and IscR regulons are responding appropriately to the resulting iron starvation. Despite the transcriptional upregulation of the enterobactin synthesis and transport systems, the siderophore is failing to accumulate in the media and is not mediating iron uptake into the cell. The results also indicate that siderophore-mediated bioremediation may be perturbed if the toxic metal, in this case nickel, also disrupts siderophore production or metabolism.

CONFLICT OF INTEREST

The authors have no conflicts of interest to declare.

DATA ACCESSIBILITY STATEMENT

The investigators will share with other researchers, at no more than incremental cost and within a reasonable time, the primary data, samples, physical collections, and other supporting materials created or gathered in the course of this work.

ORCID

Franklin W. Outten http://orcid.org/0000-0002-9095-0194

REFERENCES

Adler, C., Corbalan, N. S., Peralta, D. R., Pomares, M. F., de Cristobal, R. E., & Vincent, P. A. (2014). The alternative role of enterobactin as an oxidative stress protector allows *Escherichia coli* colony development. *PLoS ONE*, *9*, e84734. https://doi.org/10.1371/journal.pone.0084734

Albarracín, V. H., Amoroso, M. J., & Abate, C. M. (2005). Isolation and characterization of indigenous copper-resistant actinomycete strains. *Chemie der Erde-Geochemistry 65*, 145e156.

Alvarez, A., Saez, J. M., Costa, J. S. D., Colin, V. L., Fuentes, M. S., Cuozzo, S. A., … Amoroso, M. J. (2017). Actinobacteria: Current research and perspectives for bioremediation of pesticides and heavy metals. *Chemosphere*, *166*, 41–62. https://doi.org/10.1016/j.chemosphere.2016.09.070

Arnow, L. E. (1937). Colorimetric determination of the components of 3,4-di hydroxyphenylalanine-tyrosine mixtures. *Journal of Biological Chemistry*, *118*, 531–537.

Baranyi, J., & Roberts, T. A. (1994). A dynamic approach to predicting bacterial growth in food. *International Journal of Food Microbiology*, *23*, 277–294. https://doi.org/10.1016/0168-1605(94)90157-0

Bleuel, C., Grosse, C., Taudte, N., Scherer, J., Wesenberg, D., Krauss, G. J., … Grass, G. (2005). TolC is involved in enterobactin efflux across the outer membrane of *Escherichia coli*. *Journal of Bacteriology*, *187*, 6701–6707. https://doi.org/10.1128/JB.187.19.6701-6707.2005

Braud, A., Geoffroy, V., Hoegy, F., Mislin, G. L., & Schalk, I. J. (2010). Presence of the siderophores pyoverdine and pyochelin in the extracellular medium reduces toxic metal accumulation in *Psuedomonas aeruginosa* and increases bacterial metal tolerance. *Environmental Microbiology Reports*, *2*, 419–425. https://doi.org/10.1111/j.1758-2229.2009.00126.x

Braud, A., Hannauer, M., Mislin, G. L., & Schalk, I. J. (2009). The Pseudomonas aeruginosa pyochelin-iron uptake pathway and its metal specificity. *Journal of Bacteriology*, *191*, 3517–3525. https://doi.org/10.1128/JB.00010-09

Braud, A., Hoegy, F., Jezequel, K., Lebeau, T., & Schalk, I. J. (2009). New insights into the metal specificity of the Pseudomonas aeruginosa pyoverdine-iron uptake pathway. *Environmental Microbiology*, *11*, 1079–1091. https://doi.org/10.1111/j.1462-2920.2008.01838.x

Braun, V. (1995). Energy-coupled transport and signal transduction through the gram negative outer membrane via TonB-ExbB-ExbD-dependent receptor proteins. *FEMS Microbiology Reviews*, *16*, 295–307. https://doi.org/10.1111/j.1574-6976.1995.tb00177.x

Brickman, T. J., & McIntosh, M. A. (1992). Overexpression and purification of ferric enterobactin esterase from *Escherichia coli*. Demonstration of enzymatic hydrolysis of enterobactin and its iron complex. *Journal of Biological Chemistry*, *267*, 12350–12355.

Bryce, G. F., & Brot, N. (1972). Enzymic synthesis of the cyclic trimer of 2, 3-dihydroxy-N-benzoyl-L-serine in *Escherichia coli*. *Biochemistry*, *11*, 1708–1715.

Chaturvedi, K. S., Hung, C. S., Crowley, J. R., Stapleton, A. E., & Henderson, J. P. (2012). The siderophore yersiniabactin binds copper to protect pathogens during infection. *Nature Chemical Biology*, *8*, 731–736. https://doi.org/10.1038/nchembio.1020

Chen, Y., Jurkewitch, E., Bar-Ness, E., & Hadar, Y. (1994). Stability constants of pseudobactin complexes with transition metals. *Soil Science Society of America Journal*, *58*, 390–396. https://doi.org/10.2136/sssaj1994.03615999005800020021x

Crosa, J. H., & Walsh, C. T. (2002). Genetics and assembly line enzymology of siderophore biosynthesis in bacteria. *Microbiology and Molecular Biology Reviews*, *66*, 223–249. https://doi.org/10.1128/MMBR.66.2.223-249.2002

Dixit, R., Wasiullah Malaviya, D., Pandiyan, K., Sing, U. B., Sahu, A., Shukla, R., … Paul, D. (2015). Bioremediation of heavy metals from soil and aquatic environment: an overview of principles and criteria of fundamental processes. *Sustainability*, *7*, 2189–2212. https://doi.org/10.3390/su7022189

Duhme, R. C., Hider, M. J., Naldrett, M. J., & Pau, R. N. (1998). The stability of the molybdenum-azotochelin complex and its effect on siderophore production in *Azotobacter vinelandii*. *JBIC Journal of Biological Inorganic Chemistry*, *3*, 520–526. https://doi.org/10.1007/s007750050263

Ehmann, D. E., Shaw-Reid, C. A., Losey, H. C., & Walsh, C. T. (2000). The EntF and EntE adenylation domains of *Escherichia coli* enterobactin synthetase: Sequestration and selectivity in acyl-AMP transfers to thiolation domain cosubstrates. *Proceedings of the National Academy of Sciences of the United States of America*, *97*, 2509–2514. https://doi.org/10.1073/pnas.040572897

Escolar, L., Perez-Martin, J., & de Lorenzo, V. (1998). Coordinated repression in vitro of the divergent *fepA-fes* promoters of *Escherichia coli* by the iron uptake regulation (Fur) protein. *Journal of Bacteriology*, *180*, 2579–2582.

Furrer, J. L., Sanders, D. N., Hook-Barnard, I. G., & McIntosh, M. A. (2002). Export of the siderophore enterobactin in *Escherichia coli*: involvement of a 43 kDa membrane exporter. *Molecular Microbiology*, *44*, 1225–1234. https://doi.org/10.1046/j.1365-2958.2002.02885.x

Gault, M., Effantin, G., & Rodrigue, A. (2016). Ni exposure impacts the pool of free fe and modifies DNA supercoiling via metal-induced oxidative stress in *Escherichia coli* K-12. *Free Radical Biology and Medicine*, *97*, 351–361. https://doi.org/10.1016/j.freeradbiomed.2016.06.030

Gehring, A. M., Bradley, K. A., & Walsh, C. T. (1997). Enterobactin biosynthesis in *Escherichia coli*: isochorismate lyase (EntB) is a bifunctional enzyme that is phosphopantetheinylated by EntD and then acylated by EntE using ATP and 2,3-dihydroxybenzoate. *Biochemistry*, *36*, 8495–8503. https://doi.org/10.1021/bi970453p

Gehring, A. M., Mori, I., & Walsh, C. T. (1998). Reconstitution and characterization of the *Escherichia coli* enterobactin synthetase from EntB, EntE, and EntF. *Biochemistry*, *37*, 2648–2659. https://doi.org/10.1021/bi9726584

Giel, J. L., Rodionov, D., Liu, M., Blattner, F. R., & Kiley, P. J. (2006). IscR-dependent gene expression links iron-sulphur cluster assembly to the control of O_2-regulated genes in *Escherichia coli*. *Molecular Microbiology*, *60*, 1058–1075. https://doi.org/10.1111/j.1365-2958.2006.05160.x

Greenwood, K. T., & Luke, R. K. (1978). Enzymatic hydrolysis of enterochelin and its iron complex in *Escherichia coli* K-12. Properties of enterochelin esterase. *Biochimica et Biophysica Acta*, *525*, 209–218. https://doi.org/10.1016/0005-2744(78)90216-4

Hantke, K. (1990). Dihydroxybenzolyserine—a sider ophore for *E. coli*. *FEMS Microbiology Letters*, *67*, 5–8.

Hu, X., & Boyer, G. L. (1996). Siderophore-mediated aluminum uptake by *Bacillus megaterium* ATCC 19213. *Applied and Environment Microbiology*, *62*, 4044–4048.

Hunt, M. D., Pettis, G. S., & McIntosh, M. A. (1994). Promoter and operator determinants for fur-mediated iron regulation in the bidirectional *fepA-fes* control region of the *Escherichia coli* enterobactin gene system. *Journal of Bacteriology*, *176*, 3944–3955. https://doi.org/10.1128/jb.176.13.3944-3955.1994

Itoh, Y., Sugita-Konishi, Y., Kasuga, F., Iwaki, M., Hara-Kudo, Y., Saito, N., … Kumagai, S. (1998). Enterohemorrhagic *Escherichia coli* O157: H7 present in radish sprouts. *Applied and Environment Microbiology*, *64*, 1532–1535.

Kaewkla, O., & Franco, C. M. M. (2013). Rational approaches to improving the isolation of endophytic actinobacteria from Australian native trees. *Microbial Ecology*, *65*, 384–393. https://doi.org/10.1007/s00248-012-0113-z

Kieser, T., Bibb, M. J., Buttner, M. J., Chater, K. F., & Hopwood, D. A. (2000). *Practical Streptomyces Genetics*. Norwich: JIF.

Koh, E., Hung, C. S., Parker, K. S., Crowley, J. R., Giblin, D. E., & Henderson, J. P. (2015). Metal selectivity by the virulence-associated yersiniabactin metallophore system. *Metallomics*, *7*, 1011–1022. https://doi.org/10.1039/C4MT00341A

Kumar, V., Mishra, R. K., Kaur, G., & Dutta, D. (2017). Cobalt and nickel impair DNA metabolism by the oxidative stress independent pathway. *Metallomics*, *9*, 1596–1609. https://doi.org/10.1039/C7MT00231A

Langman, L., Young, I. G., Frost, G. E., Rosenberg, H., & Gibson, F. (1972). Enterochelin system of iron transport in *Escherichia coli*: mutations affecting ferric-enterochelin esterase. *Journal of Bacteriology*, 112, 1142–1149.

Larsen, R. A., Foster-Hartnett, D., McIntosh, M. A., & Postle, K. (1997). Regions of *Escherichia coli* TonB and FepA proteins essential for in vivo physical interactions. *Journal of Bacteriology*, 179, 3213–3221. https://doi.org/10.1128/jb.179.10.3213-3221.1997

Lin, H., Fischbach, M. A., Liu, D. R., & Walsh, C. T. (2005). In vitro characterization of salmochelin and enterobactin trilactone hydrolases IroD, IroE, and Fes. *Journal of the American Chemical Society*, 10, 11075–11084. https://doi.org/10.1021/ja0522027

Ma, L., & Payne, S. M. (2012). AhpC is required for optimal production of enterobactin by *Escherichia coli*. *Journal of Bacteriology*, 194, 6748–6757. https://doi.org/10.1128/JB.01574-12

Macomber, L., Elsey, S. P., & Hausinger, R. P. (2011). Fructose-1,6-bisphosphate aldolase (class II) is the primary site of nickel toxicity in *Escherichia coli*. *Molecular Microbiology*, 82, 1291–1300. https://doi.org/10.1111/j.1365-2958.2011.07891.x

Macomber, L., & Hausinger, R. P. (2011). Mechanisms of nickel toxicity in microorganisms. *Metallomics*, 3, 1153–1162. https://doi.org/10.1039/c1mt00063b

Macomber, L., & Imlay, J. A. (2009). The iron-sulfur clusters of dehydratases are primary intracellular targets of copper toxicity. *Proceedings of the National Academy of Sciences of the United States of America*, 20, 8344–8349. https://doi.org/10.1073/pnas.0812808106

Matthew, A., Jenul, C., Carlier, A. L., & Eberl, L. (2016). The role of siderophores in metal homeostasis of members of the genus *Burkholderia*. *Environmental Microbiology Reports*, 8, 103–109. https://doi.org/10.1111/1758-2229.12357

Miethke, M., Hou, J., & Marahiel, M. A. (2011). The siderophore-interacting protein YqjH acts as a ferric reductase in different iron assimilation pathways of *Escherichia coli*. *Biochemistry*, 50, 10951–10964. https://doi.org/10.1021/bi201517h

Miethke, M., & Marahiel, M. A. (2007). Siderophore-based iron acquisition and pathogen control. *Microbiology and Molecular Biology Reviews*, 71, 413–451. https://doi.org/10.1128/MMBR.00012-07

Miller, J. H. (1972). *Experiments in molecular genetics*. Cold Spring Harbory, NY: Cold Spring Harbor Laboratory.

Nair, P. K. (2007). The coming of age of agroforestry. *Journal of the Science of Food and Agriculture*, 87, 1613–1619. https://doi.org/10.1002/(ISSN)1097-0010

Neilands, J. B. (1995). Siderophores: structure and function of microbial iron transport compounds. *Journal of Biological Chemistry*, 270, 26723–26726. https://doi.org/10.1074/jbc.270.45.26723

O'Brien, I. G., & Gibson, F. (1970). The structure of enterochelin and related 2,3-dihydroxy-n-benzoylserine conjugates from *Escherichia coli*. *Biochimica et Biophysica Acta*, 215, 393–402. https://doi.org/10.1016/0304-4165(70)90038-3

Polti, M., Amoroso, M., & Abate, C. (2011). Intracellular chromium accumulation by *Streptomyces* sp. MC1. *Water, Air, and Soil pollution*, 214, 49–57. https://doi.org/10.1007/s11270-010-0401-5

Polti, M., Aparicio, J. D., Benimeli, C. S., & Amoroso, M. J. (2014). Simultaneous bioremediation of Cr(VI) and lindane in soil by actinobacteria. *International Biodeterioration and Biodegradation*, 88, 48–55. https://doi.org/10.1016/j.ibiod.2013.12.004

Polti, M. A., Atjian, M. C., Amoroso, M. J., & Abate, C. M. (2011). Soil chromium bioremediation: synergic activity of actinobacteria and plants. *Int. Biodeterior. Biodegrad.*, 65, 1175–1181. https://doi.org/10.1016/j.ibiod.2011.09.008

Polti, M. A., García, R. O., Amoroso, M. J., & Abate, C. M. (2009). Bioremediation of chromium(VI) contaminated soil by Streptomyces sp. MC1. *Journal of Basic Microbiology*, 49, 285–292. https://doi.org/10.1002/jobm.200800239

Ranquet, C., Ollagnier-de-Choudens, S., Loiseau, L., Barras, F., & Fontecave, M. (2007). Cobalt stress in *Escherichia coli*: The effect on the iron-sulfur proteins. *Journal of Biological Chemistry*, 282, 30442–30451. https://doi.org/10.1074/jbc.M702519200

Rolfe, M. D., Rice, C. J., Lucchini, S., Pin, C., Thompson, A., Cameron, A. D., … Hinton, J. C. (2012). Lag phase is a distinct growth phase that prepares bacteria for exponential growth and involves transient metal accumulation. *Journal of Bacteriology*, 194, 686–701. https://doi.org/10.1128/JB.06112-11

Roth, V. (2006). Doubling Time. (http://www.doubling-time.com/compute.php)

Shaw-Reid, C. A., Kelleher, N. L., Losey, H. C., Gehring, A. M., Berg, C., & Walsh, C. T. (1999). Assembly line enzymology by multimodular non-ribosomal peptide synthetases: the thioesterase domain of *E. coli* EntF catalyzes both elongation and cyclolactonization. *Chemistry & Biology*, 6, 385–400. https://doi.org/10.1016/S1074-5521(99)80050-7

Solomon, E. B., Yaron, S., & Matthews, K. R. (2002). Transmission of *Escherichia coli* O157:H7 from contaminated manure and irrigation water to lettuce plant tissue and its subsequent internalization. *Applied and Environment Microbiology*, 68, 397–400. https://doi.org/10.1128/AEM.68.1.397-400.2002

Van Elsas, J. D., Semenov, A. V., Costa, R., & Trevors, J. T. (2011). Survival of *Escherichia coli* in the environment: fundamental and public health aspects. *ISME Journal*, 5, 173–183. https://doi.org/10.1038/ismej.2010.80

Visca, P., Colotti, G., Serino, L., Verzili, D., Orsi, N., & Chiancone, E. (1992). Metal regulation of siderophore synthesis in *Pseudomonas aeruginosa* and functional effects of siderophore-metal complexes. *Applied and Environment Microbiology*, 58, 2886–2893.

Wade, H. E. (1952). Observations on the growth phases of *Escherichia coli*, American Type 'B'. *Journal of General Microbiology*, 7, 18–23. https://doi.org/10.1099/00221287-7-1-2-18

Walsh, C. T., Liu, J., Rusnak, F., & Sakaitani, M. (1990). Molecular studies on enzymes in chorismate metabolism and the enterobactin biosynthetic pathway. *Chemical Reviews*, 90, 1105–1129. https://doi.org/10.1021/cr00105a003

Wang, W., Qiu, Z., Tan, H., & Cao, L. (2014). Siderophore production by actinobacteria. *BioMetals*, 27, 623–631. https://doi.org/10.1007/s10534-014-9739-2

Wang, S., Wu, Y., & Outten, F. W. (2011). Fur and the novel regulator YqjI control transcription of the ferric reductase gene *yqjH* in *Escherichia coli*. *Journal of Bacteriology*, 193, 563–574. https://doi.org/10.1128/JB.01062-10

Xu, F. F., & Imlay, J. A. (2012). Silver(I), mercury(II), cadmium(II), and zinc(I) target exposed enzymic iron-sulfur clusters when they toxify *Escherichia coli*. *Applied and Environment Microbiology*, 78, 3614–3621. https://doi.org/10.1128/AEM.07368-11

SUPPORTING INFORMATION

Additional supporting information may be found online in the Supporting Information section at the end of the article.